

Modeling of magnetic tunnel junctions with multidomain ferromagnetic layers

P. K. Wong, J. E. Evetts, and M. G. Blamire

Department of Materials Science and Metallurgy, University of Cambridge, Pembroke Street, Cambridge CB2 3QZ, United Kingdom

(Received 4 March 1999)

A statistical model of ferromagnet-insulator-ferromagnet (FM-I-FM) tunnel junctions based on the multidomain nature of the FM layers has been developed. It expresses the explicit relationship between the junction magnetoresistance (MR) and the magnetizations of the FM electrodes. Analysis based on the model revealed the important role of antiferromagnetic interaction of the electrodes in the formation of MR peaks. The model also implies the decrease of MR with temperature through its effect on the magnetism of the FM layers.

I. INTRODUCTION

A. Background

Over the twenty years since the pioneering work of Julliere,¹ study of the magnetoresistive (MR) behavior of ferromagnet-insulator-ferromagnet (FM-I-FM) tunneling has been focused on the fabrication aspects, especially on the improvement of the tunnel barrier. Effort on modeling the phenomena was relatively modest, although there were large differences between the two early models proposed by Julliere¹ and Slonczewski.² Moreover there were puzzles of the temperature and bias voltage dependence of the observed MR.^{3,4} A major reason for the lack of theoretical studies was the unavailability of high-quality FM-I-FM junctions, hindering the comparison between theory and observation. Throughout these two decades, the MR observed in various FM-I-FM systems was restricted to a few percent, casting doubts on the validity of Julliere's model which predicted a temperature-independent tunneling MR of over 20%. A breakthrough in MR value came in 1995 when Moodera *et al.* reported 10.8% at 295 K and 24% at 4.2 K in CoFe/Al₂O₃/Co junctions,⁵ in support of Julliere's prediction of 27% for CoFe-I-Co systems. Since then, more results of high MR values have been published and now over 20% is achievable even at room temperature.^{6,7} Findings from such high-quality junctions recently sparked a number of theoretical studies into the mechanism of spin-dependent tunneling.⁷⁻¹⁴

The response of junction MR to temperature and bias voltage provides important clues to the origin of the phenomenon, and has been the subject of the recent theoretical studies. Although Julliere provided an useful link between the tunneling MR and the electron spin polarizations of the ferromagnets, and has recently gained support from the high MR reported, it is considered oversimplified for the problem of temperature and voltage effects. Theories which attempted to explain the phenomenon at the electronic level, assumed the FM-I-FM tunnel junction to be a sandwich structure with an insulator between two ferromagnetic layers, magnetically and electronically homogeneous across the plane normal to the tunnel current. However, in actual junctions, the FM layers are unlikely to possess single domain structures. Nowak and Rauluszkiwicz¹⁵ studied Fe/GdO_x/Fe junctions by electron microscopy and found that the Fe electrodes consisted of micron size magnetic domains. Even for junction areas

down to submicron scale,¹⁶ multidomain structure still exist. The links between such domain structure and the MR behavior, including the temperature and bias voltage dependency, has not been explored. In this paper, we report a statistical model to describe the multidomain effects in magnetic tunnel junctions, with comparisons to our own data and those from junctions showing the record high MR values.^{5,6} Our model suggests that the MR of a ferromagnetic junction as a function of an applied field is closely related to the domain alignments in the FM layers. Moreover, the domain structure also contributes to the temperature dependence of MR. Further analyses also revealed the process and importance of antiferromagnetic interaction of the FM electrodes in the formation of MR peaks.

B. Definition and notations of MR

We first clarify the definitions of MR and some notations we have used in this paper. We refer MR of a junction to the percentage change of resistance with respect to the resistance at high magnetic field. Moreover we have used the leakage conductance model¹⁷ in the discussion, which involved three notations of MR: The first is the MR actually observed in measurements, denoted by w_{obs} , which is affected by the presence of ohmic leakage through the tunnel barrier. The second one, denoted by w , is the MR expected from a similar but leakage-free junction. Both w_{obs} and w are functions of applied field (H), temperature (T), and bias voltage. Thirdly, w^* represents the highest possible MR value between antiparallel and parallel orientations of the magnetizations of the FM electrodes. Therefore w^* is independent of the applied field H . In real junctions, a hypothetical leakage-free junction is assumed to be electrically parallel to a leakage path. Then the MR measured can be written as

$$w_{\text{obs}} = \frac{(G_{\text{hf}} + G_l) - (G_p + G_l)}{G_p + G_l}, \quad (1)$$

where G_{hf} and G_p are the conductance of the leakage-free junction at high field and at the MR peak, respectively. G_l is the conductance of the leakage path. The MR of the leakage-free junction is defined as

$$w = \frac{G_{\text{hf}} - G_p}{G_p}. \quad (2)$$

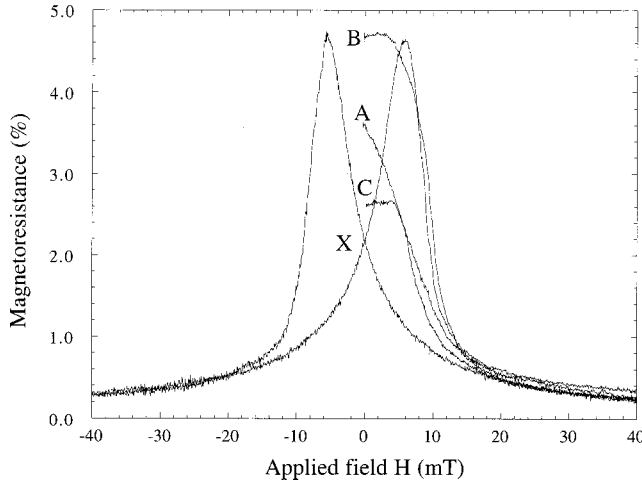


FIG. 1. The initial MR- H curves and the hysteretic peaks. X, A, B and C, are MR values at zero applied field (i.e., MR_0) for $t_H=0$ min, 2 min, 30 min, and 2 days at 300 K.

By putting Eq. (2) into Eq. (1), the expression of the leakage conductance model is obtained:

$$w_{\text{obs}} = \left(\frac{G_p}{G_p + G_l} \right) w. \quad (3)$$

From Eq. (3), w_{obs} is directly proportional to w . The proportional constant $G_p/(G_p + G_l)$ is called the leakage factor. The multidomain model derived below gives the linkage between w and w^* , which is the highest possible MR value.

C. The MR- H curves

Here we present features of the MR- H curves measured with our FM-I-FM junctions. Results described here serve as an experimental test of the multidomain model derived in the next section. We have studied $8 \times 8 \mu\text{m}^2$ Fe/Al₂O₃/CoFe mesa junctions defined by photolithography on sputtered Nb/Fe/Al₂O₃-Al/CoFe/Nb multilayers. The alumina barrier was prepared by the multiple oxidation technique, giving a small resistance-area product of $10^3 \Omega \mu\text{m}^2$, corresponding to a barrier with three extra Al₂O₃ layers.¹⁷ Details of the fabrication process and the electrical properties of the junctions have been reported elsewhere.¹⁷ Figure 1 shows a typical MR- H curve obtained in a magnetic-field cycle. The hysteretic MR peaks are positioned between the coercive fields of the FM layers. The low and saturated resistance at high field corresponds to parallel alignment of the magnetizations, while the peak between the coercivities corresponds to partially antiparallel alignment. Initial MR- H curves, which started from $H=0$ to the saturation field, have been observed (also shown in Fig. 1), with starting points at A, B, and C. Before measuring the initial curves, the sample was left in zero field for a period of time t_0 after the previous magnetic cycle. A, B, and C corresponded to t_0 of 2 min, 30 min, and 2 days, respectively. The variation of MR at zero field (MR_0) upon t_0 at room temperature was found as follows: immediately after the magnetic cycle (i.e., $t_0=0$), MR_0 equalled the zero-field value of the hysteretic MR- H curve (point X in Fig. 1); then MR_0 rose gradually to its highest value which was 1–1.09 times of the peak value (MR_{peak}) in

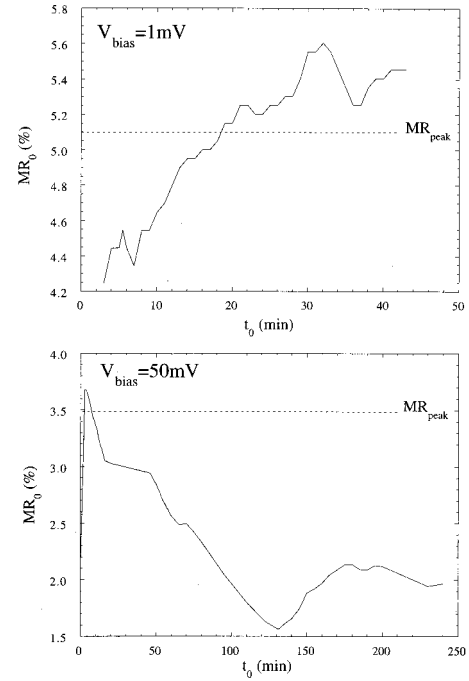


FIG. 2. The changes of MR_0 with $t_H=0$ in the first 42 min and 250 min.

20–30 min (point B); finally it decayed very slowly to a steady value (point C) in about 2 days. The steady value was about 40–60% of MR_{peak} . Figure 2 showed examples of MR_0 against t_0 . Initial curves starting from the highest (point B) and the steady (point C) values had flat tops up to ≈ 3 mT, showing insensitivity to small field variations. Initial curves starting from other locations (e.g., point A) did not have flat tops. We also observed the variation of MR_0 with t_0 at 77 K. The magnetic cycle in LN₂, MR_0 was found frozen at a value slightly higher than the hysteretic curve (point X) throughout the 2 h duration of experiment. Such freezing effect was also observed with various t_0 when the LN₂ cooling was started. We conclude that the change of MR_0 with t_0 is sensitive to temperature and that low temperature can significantly slow down the change. The effect of bias voltage has also been explored. In general, it was more difficult for MR_0 to rise beyond the peak value with a high bias voltage, and the flat top in low field has not been observed in high bias cases. In addition, the ratio of maximum MR_0 (e.g. point B of Fig. 1) to the peak value MR_{peak} decreases slightly with voltage (Fig. 3).

II. THE MULTIDOMAIN MODEL

In the light of the above experimental results, we propose that the variation of MR_0 with t_0 results from changes in the alignment of magnetic domains in the FM layers. We further assume that the layers consist of a large number of small domains with equal magnitude of spontaneous magnetization, and each domain has homogeneous, magnetic, and electronic properties. For simplicity we assume that the magnetizations are in-plane, and resolve them into orthogonal directions with H as the reference direction. There are at least two justifications: first, H in MR measurements are usually in-plane; secondly, it is demagnetization effects that

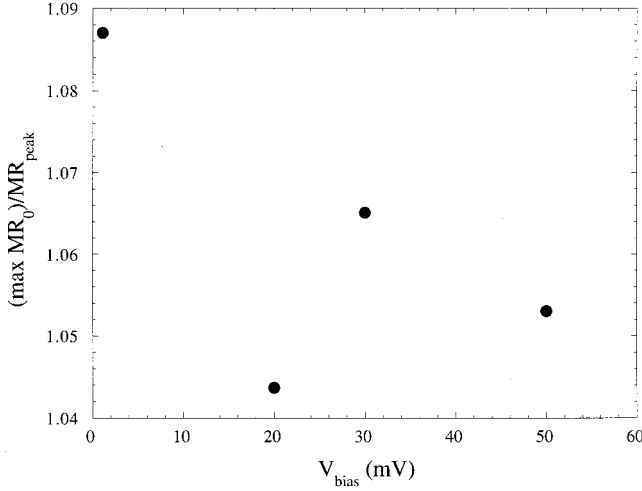


FIG. 3. The ratio of maximum MR value of the initial curve ($\max MR_0$) to the MR at the hysteretic peak (MR_{peak}) decreases with bias voltage (V_{bias}).

make it energetically more favorable for the magnetizations to lie along a thin film. Figure 4 shows the schematic division of the FM layers into domains with magnetizations in the directions indicated by the arrows. a_i and b_i are the proportions of domains lying in a particular direction in the top and bottom layers, respectively. By convention $0 \leq a_i, b_i \leq 1$ and $\sum a_i = \sum b_i = 1$. The idea is that an electron in one electrode has a finite probability of tunneling into a domain bearing one of the four possible magnetization directions, and thus four possible tunneling conductivities. Here MR is defined as

$$w(H, T) = \frac{R(H, T) - R_p}{R_p} = \frac{G_p}{G(H, T)} - 1 \quad (4)$$

where R and G denote the resistance and conductance of the junction, respectively. R_p (G_p) is the resistance (conductance) of the junction when the magnetizations are in parallel. The conductance $G(H, T)$ is the sum of the conductance due to tunneling between various domains. To calculate $G(H, T)$, we consider a simple case that there is negligible magnetic interaction between the FM layers. In other words, the distributions of a_i and b_i are statistically independent of each other. In Sec. III, we will compare our model with

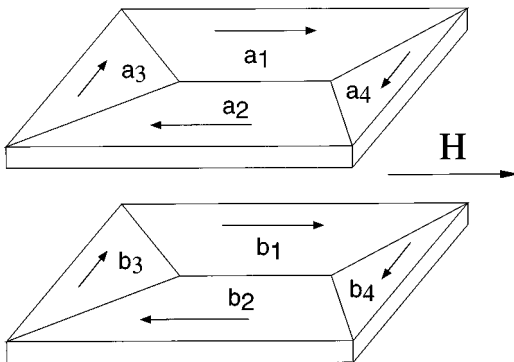


FIG. 4. Geometry of the model, a_i and b_i are the proportions of the domains lying in direction indicated by the arrows in the top and bottom layers, respectively.

experimental MR- H curves, and the effect of magnetic interaction will be discussed. The tunneling probabilities are then proportional to that of an electron seeing certain magnetization on the other side of the barrier. By putting $a_{\perp} = a_3 = a_4$ and $b_{\perp} = b_3 = b_4$, and writing $G(H, T)$ in terms of the tunneling probabilities,

$$G(H, T) = g(a_1 b_2 + a_2 b_1 + 2a_{\perp} b_{\perp}) + g(1 + w^*) \\ \times (a_1 b_1 + a_2 b_2 + 2a_{\perp} b_{\perp}) + g \left(1 + \frac{w^*}{2} \right) \\ \times (2a_1 b_{\perp} + 2a_2 b_{\perp} + 2b_1 a_{\perp} + 2b_2 a_{\perp}), \quad (5)$$

where g is the theoretical tunneling conductance between antiparallel magnetizations and w^* is the theoretical peak MR. $g(1 + w^*)$ is the theoretical conductance between parallel magnetizations, and $g(1 + w^*/2)$ is the conductance between orthogonal magnetizations suggested by Slonczewski's calculation on the angular dependence of tunneling MR.² In high enough field, the magnetisations will be saturated and in parallel, i.e., $a_1 = b_1 = 1$. Then we have $G_p = g(1 + w^*)$. Substituting G_p and Eq. (5) into Eq. (4),

$$(1 + w) = \frac{G_p}{G(H, T)} = \frac{(1 + w^*)}{(uw^* + 1)} \quad (6)$$

where $u = a_{\perp} + a_1(b_1 + b_{\perp}) + a_2(b_2 + b_{\perp})$, which contains the information about the domain alignments and is a function of H and T . Here we introduce the normalized magnetizations M_a/M_{as} and M_b/M_{bs} of the top and bottom electrodes, respectively. M_a (M_b) is the magnetization of the top (bottom) electrode and M_{as} (M_{bs}) is the saturated magnetization. By writing $M_a/M_{as} = a_1 - a_2$ and $M_b/M_{bs} = b_1 - b_2$, u can then be expressed in terms of the normalized magnetizations as

$$u = \frac{1}{2} \left[1 + \left(\frac{M_a}{M_{as}} \right) \left(\frac{M_b}{M_{bs}} \right) \right]. \quad (7)$$

Since $-1 \leq M_a/M_{as}, M_b/M_{bs} \leq 1$, u is within the range $0 \leq u \leq 1$. At high field, $M_a/M_{as} = M_b/M_{bs} = \pm 1$ and so $u = 1$, giving $w = 0$ from Eqs. (6) and (7). For the highest possible MR, the magnetizations of the FM are antiparallel, i.e., $(M_a/M_{as})(M_b/M_{bs}) = -1$ and $u = 0$, giving $w = w^*$, which is the theoretical peak MR value.

The evolution of the initial MR- H curves can be interpreted with the multidomain model as follows: At $t_0 = 0$, the FM layers possess parallel remanent magnetizations such that $0 < |M_a/M_{as}|, |M_b/M_{bs}| < 1$, giving a MR halfway between MR_{peak} and the value at high field (i.e. point X in Fig. 1). This parallel alignment is energetically unfavorable and so the domains rearrange to form a partially antiferromagnetic (AF) configuration in order to reduce the magnetostatic stray fields. AF configuration corresponds to $(M_a/M_{as})(M_b/M_{bs}) = -1$, giving the highest possible MR value (MR_{max}) as calculated from Eqs. (6) and (7) (i.e. point B in Fig. 1). The peak value (MR_{peak}) was only slightly lower ($MR_{\text{max}}/MR_{\text{peak}} = 1 - 1.09$) than the maximum value of the initial curve, implying substantial AF alignment at the peak field. A complete enclosure of flux cannot be achieved by the AF alignment, but by forming closed loops within each FM layer. This happens when $M_a/M_{as} = M_b/M_{bs} = 0$ (i.e.,

point C in Fig. 1), and so $u=0.5$ and $MR_0/MR_{\text{peak}}=w/w^*=(2+w^*)^{-1}$. Taking the electron spin polarizations of CoFe and Fe to be 47% and 40%, respectively, w^* found with Julliere's model (using our definition of MR) is 46.3%, resulting in $w/w^*=0.41$ (or 41%). This value is consistent with the minimum value of steady MR_0 with $t_0 > 2$ days (MR_0/MR_{peak} is observed to be 40–60% after 2 days). That it took much longer time to reach the $M_a/M_{as}=M_b/M_{bs}=0$ state (>2 days) than to the AF state (≈ 30 min) implies a strong AF interaction between the FM layers. The flat tops of the initial curves starting from B and C in Fig. 1 confirmed that the two states are energetically more stable.

The above picture of the initial MR- H curve as a function of time (i.e., t_0) does not explain why the AF state has to come before the $M_a/M_{as}=M_b/M_{bs}=0$ state. Other experimental results actually showed that whether the MR will rise to above MR_{peak} (i.e., to the AF state in our interpretation) depends on the magnetizations of the FM layers at time zero, i.e., $t_0=0$. In an experiment, we observed the change in junction resistance (i.e., the MR) with time after the field is abruptly removed from various values during a magnetic cycling. When the field was removed: (i) from high values (i.e., when the magnetizations are parallel), the MR did not rise beyond the $M_a/M_{as}=M_b/M_{bs}=0$ state throughout the 12 hours of observation; (ii) from a narrow range of about 0–1.4 mT, the MR rose to above the peak value; (iii) from intermediate values around the width of the peak, MR rose to above the peak value only near the peak field. (i), (ii) and (iii) show that the occurrence of the AF state is highly dependent on the magnetizations of the FM layers at the beginning of the evolution. Moreover from (iii), we saw that even when the layers were already engaged in dipolar interactions (for fields between the coercivities), it did not necessarily result in the AF state. This means that although dipolar interaction is essential for the development of a complete AF configuration, it is not a sufficient condition. The strong dependence of the evolution on the initial states can be qualitatively understood by realizing that the problem involves solving two coupled differential equations of $\partial M/\partial t$ of both FM layers.

For the freezing effect at low temperature, it is simply because the rates of domain processes were lowered upon cooling. If the above describes correctly the evolution of domain ordering at zero field, it is clear that the influence of thermal agitation is significant even at room temperature. In this case, the thermal energy is mainly for overcoming the crystallographic anisotropy for the coherent rotation of domains. Such rotation is called by Néel as the thermal fluctuation aftereffect.¹⁸ Since the energy of anisotropy is proportional to the volume of the domain, for such rotation to take place the domain cannot be bigger than certain critical volume, given by $k_B T/2K_u$ where K_u is the anisotropy constant of the FM material.^{18,19} For Fe, $K_u=0.48 \times 10^5 \text{ J m}^{-3}$ (Ref. 20) and the critical volume at 295 K corresponds to a dimension of 35 Å, which is consistent with the observations in submicron ferromagnetic tunnel junctions.¹⁶

To explain the slight voltage dependence of $MR_{\text{max}}/MR_{\text{peak}}$ (see Fig. 3), we substituted Eq. (7) into Eq. (6) to get $w=w^*(1-u)/(uw^*+1)$. MR_{max} corresponds to the AF alignment (i.e., $u=0$) and so $MR_{\text{max}}=sw^*$, where s was the leakage factor mentioned in Sec. I. Similarly,

$MR_{\text{peak}}=sw^*(1-u_{\text{peak}})/(u_{\text{peak}}w^*+1)$. By putting the expressions together, $MR_{\text{max}}/MR_{\text{peak}}=(u_{\text{peak}}w^*+1)/(1-u_{\text{peak}})$. Since the bias voltage does not affect the magnetic alignment represented by u_{peak} , the decrease of $MR_{\text{max}}/MR_{\text{peak}}$ ratio was clearly a result of w^* reduction due to increased bias voltage. Besides, since $u_{\text{peak}} \leq 1$, the dependence of $MR_{\text{max}}/MR_{\text{peak}}$ on voltage was smaller than that of w^* itself.

The expression $MR_{\text{max}}/MR_{\text{peak}}=(u_{\text{peak}}w^*+1)/(1-u_{\text{peak}})$ provides a way to estimate the normalized magnetizations (M/M_s) of the FM electrodes at the peak, which is difficult to measure directly in a tunnel junction structure. As an example, we have put $MR_{\text{max}}/MR_{\text{peak}}=1-1.09$ from our measurement and $w^*=0.463$ (46.3%) calculated with Julliere's formula. $u_{\text{peak}}=0-0.06$ was then obtained, and from Eq. (7), $M/M_s \approx 0.94-1$. These values of M/M_s was higher than those of individual (i.e., uncoupled) CoFe and Fe thin films at the peak field, implying the existence of AF interaction. A more detailed discussion on AF interaction is given in the next section. To conclude this section, the multidomain model gives a good account of the behavior of the initial MR- H curves.

III. SIMULATION OF MR PEAKS

Equations (6) and (7) suggested an explicit relationship between MR values and the magnetizations of the FM electrodes. Such relationship is useful for understanding the formation of features in the MR peak. In this section, the hysteretic MR peaks of FM-I-FM junctions were simulated using Eqs. (6) and (7) with the knowledge of the magnetizations of the individual FM layers.

We have simulated the MR- H curves of the CoFe/Al₂O₃/Fe junctions in Ref. 5 and the Ni/Al₂O₃/Co junctions in Ref. 21. The two reasons of choosing these results are the following: First, information of the magnetizations was given in these articles [note the authors of Ref. 5 used a different definition of MR in their article. The data quoted here are transformed with our definition in Eq. (2)]. Secondly, Refs. 5 and 21 are examples of very high and very low MR, respectively. The following analysis shows that the large difference in MR was caused not only by the large difference in barrier leakage, but also by the different degree of AF interaction in the magnetization alignments. The w^* values used in the simulations were 0.38 (38%) for CoFe/Al₂O₃/Co and 0.175 (17.5%) for Ni/Al₂O₃/Co as calculated from Julliere's model with spin polarizations quoted from the literature.^{5,22} Figure 5 shows the simulated data points and the original MR peaks. For the Ni/Al₂O₃/Co junctions, the simulation was in good agreement with experimental MR- H curves. For the CoFe/Al₂O₃/Fe junctions, excellent agreement was achieved for regions with MR=4.5%. The proportionality of the simulated points and the experimental curves was readily explained by the leakage conduction model mentioned in Sec. I.

In the derivation in Sec. II, we have assumed that the FM layers acted independently in an applied field, i.e., without any AF interaction. This assumption was also applied in the above two simulations because we employed the magnetization curves of the individual FM films. Therefore the agreement between simulated data and the measured one in the

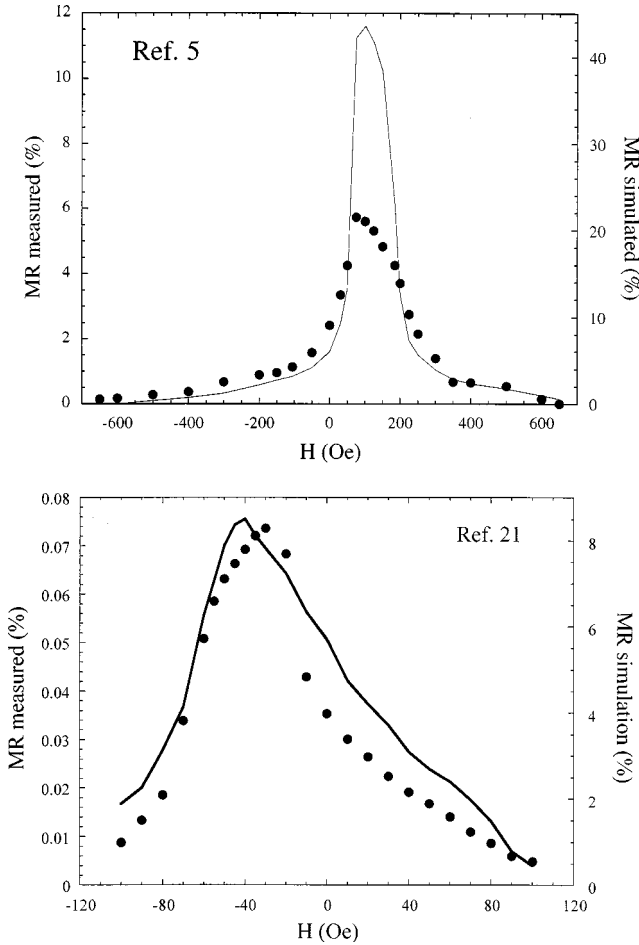


FIG. 5. Simulations of MR- H curves for CoFe/Al₂O₃/Co junctions of Ref. 5 and Ni/Al₂O₃/Co of Ref. 21. The solid lines are the measured curves and ● are values calculated with the multidomain model.

Ni/Al₂O₃/Co junctions meant that the Ni and Co layers had little AF interaction in the reversal process. Such uncoupled magnetization reversal process resulted in a less rapid change of MR along the two sides of the peak. For the CoFe/Al₂O₃/Fe junctions, we have plotted in Fig. 6 the experimental MR values against the corresponding simulated ones. A sharp switch of slope occurred when the simulated MR equals 16% (or 4.5% for the experimental value), which marked a sharp onset of AF interaction. The sharp change corresponded to $H=55$ and 192 Oe, very close to the coercivities of Co (53.5 Oe) and CoFe (193 Oe).⁵ Therefore, in this case AF interaction occurred between the coercivities, and the interaction promoted the formation of steep edges of the MR peak. This challenges the common idea that single domain structure (or high squareness of magnetization) was essential for forming steep and flat topped MR peaks.

IV. AF INTERACTION IN FM-I-FM JUNCTIONS

The steepness on the sides (i.e., high MR/ H sensitivity) and flatness on the top (i.e., a “saturated” state) are desirable for the applications of FM-I-FM junctions in field sensing and magnetic storage. This motivated us to make a further examination of the AF interaction in FM-I-FM junctions. First, we would like to introduce an easy way to

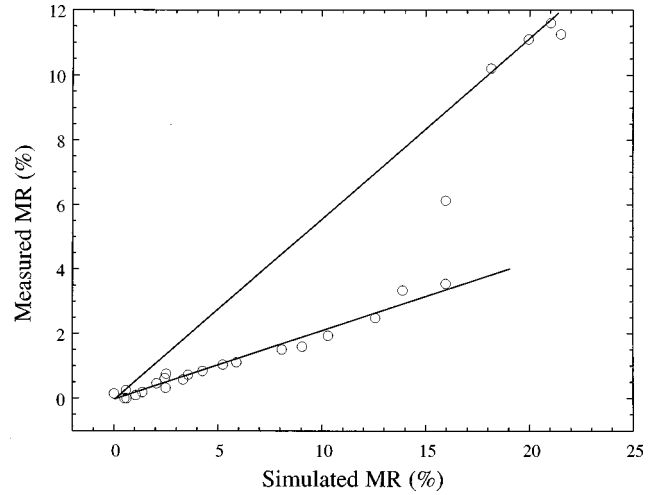


FIG. 6. The experimental MR values of CoFe/Al₂O₃/Co junctions in Ref. 5 are plotted against the simulated values calculated from the magnetization curves of CoFe and Fe electrodes reported in the same article.

check whether AF interaction has taken place beyond the coercive fields. Precise knowledge of the magnetizations is unnecessary, which is an advantage of the method. Considering no AF interaction at H_c of either FM electrodes, then M/M_s vanish and from Eq. (7) $u=0.5$ at both H_c . By putting $u=0.5$ into Eq. (6), we have $w=w^*/(w^*+2)$ at both H_c . So the ratio w/w_{peak} at both H_c will be

$$\frac{w}{w_{\text{peak}}} = \frac{u_{\text{peak}}w^* + 1}{(1 - u_{\text{peak}})(w^* + 2)}. \quad (8)$$

If there is substantial interaction at the MR peak, then $u_{\text{peak}} \approx 0$ and

$$\frac{w}{w_{\text{peak}}} \approx \frac{1}{w^* + 2}. \quad (9)$$

We have applied Eq. (9) to the CoFe/Al₂O₃/Co and Co/Al₂O₃/Ni₈₀Fe₂₀ junctions of Moodera and co-workers,^{5,6} which are junctions with the highest field sensitivity and highest peak MR values, respectively, reported so far. w^* were 0.38 (38%) for the CoFe/Al₂O₃/Co system and 0.374 (37.4%) for the Co/Al₂O₃/Ni₈₀Fe₂₀ system, as calculated with the spin polarizations quoted in the original articles. So w/w_{peak} at H_c are 0.42 for both cases. We then drew the lines $\text{MR}=0.42\text{MR}_{\text{peak}}$ across the MR peaks (the 295 K ones) quoted in the articles and the intersections should correspond to the H_c values if there was no AF interaction at the coercivities. The H_c found by this method are 198 Oe for CoFe and 62 Oe for Co in the CoFe/Al₂O₃/Co junctions (cf. 193 Oe and 53.5 Oe for CoFe and Co, respectively, in Ref. 5, and 20.8 Oe for Co and 5.4 Oe for Ni₈₀Fe₂₀ in the Co/Al₂O₃/Ni₈₀Fe₂₀ junctions (cf. ≈ 25 Oe and ≈ 5 Oe for Co and Ni₈₀Fe₂₀, respectively in Ref. 6), which agreed well with literature values. To conclude, in both cases AF interaction was not significant at fields beyond the coercivities of the electrodes. The steep edges of the MR peaks were probably due to the sharp onset of the AF effect instead of the magnetic switching of individual FM layers.

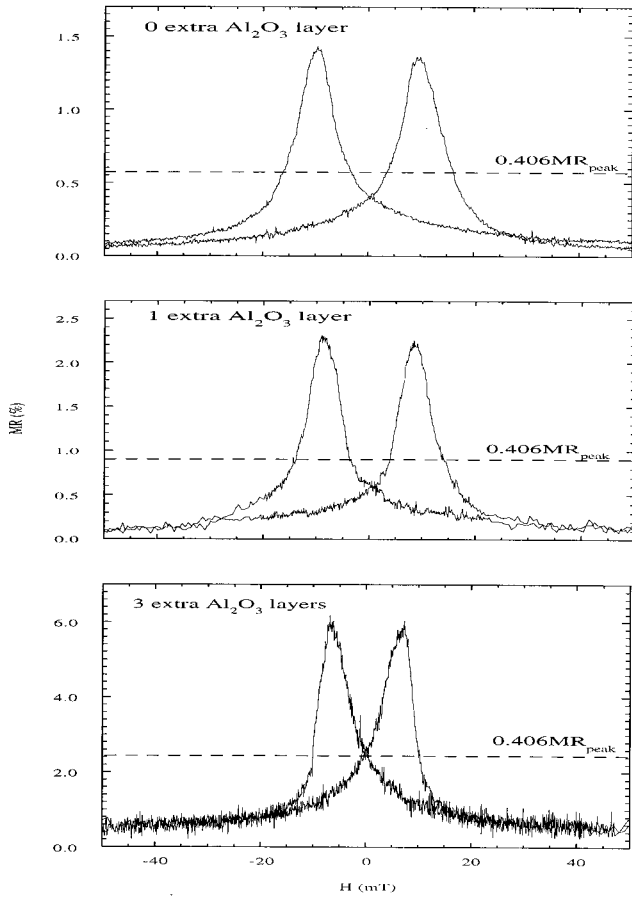


FIG. 7. MR peaks of Fe/Al₂O₃/CoFe junctions with 0, 1, and 3 extra Al₂O₃ layers in their multiply oxidized barriers.

We have also carried out the above analysis for our Fe/Al₂O₃/CoFe junctions with multiply oxidized barrier. In such barriers, an about 1 nm Al layer was first deposited and oxidized in 1 kPa O₂ for 10 min. Then extra thin layers of Al were deposited on top, each followed by 10 min of oxidation in 1 kPa O₂. Finally, the whole barrier was oxidized for 1 h with the same O₂ pressure. By increasing the number of extra Al₂O₃ layers, leakage through pinholes could be progressively reduced. A detailed description of the barrier preparation can be found in Ref. 17. In the present analysis, we used junctions with 0, 1, and 3 extra Al₂O₃ layers. Figure 7 showed the MR peaks of the three kinds of junctions at room temperature. Those with 0 and 1 extra Al₂O₃ layer were proportionally similar to each other, and the 3-layer one was more different from others. By putting $w^* = 0.463$ (46.3%) into Eq. (9), we obtained $w/w_{\text{peak}} = 0.406$ at both H_c . Constructions of the $\text{MR} = 0.406\text{MR}_{\text{peak}}$ lines across the peaks were also shown in Fig. 7. The coercivities resulted from the constructions and also the values measured with individual Fe and CoFe thin films are listed in Table I. The 0 and 1 layer cases were in good agreement with values from individual thin films. Therefore the AF interaction in these two kinds of junctions was insignificant in regions beyond the coercivities.

For the junctions with 3 extra Al₂O₃ layers, the construction did not reveal the correct coercivities, implying that there was appreciable interaction between the FM layers. We

TABLE I. Summary of the coercivities of Fe and CoFe in Fe/Al₂O₃/CoFe junctions found by the multidomain model. The tunnel barriers were prepared by the multiple oxidation method.

Number of extra Al ₂ O ₃ layers in barrier	H_c of Fe (Oe)	H_c of CoFe (Oe)
0	34	162
1	36	143
3	0	101
H_c of individual thin films		40
		156

have compared our MR peaks with those reported by Tsuge and Mitsuzuka,²³ which have the same FM layers, similar resistance-area products and highly similar peak shapes as ours. Tsuge and Mitsuzuka have performed an analysis on the relation between the zero-field junction resistance and the area of the FM electrodes, and concluded that there was significant AF interaction of the electrodes even at low-field regions due to the magnetostatic fields generated at the junction edges.²³ Their conclusion was the same as ours from the analysis with the multidomain model. However, in addition to their argument in terms of junction area, we found that a difference in barrier properties may also affect the occurrence of AF interaction as all our junctions possessed the same area.

Although AF interaction leads to favourable features in FM-I-FM junctions for magnetic sensing and storage, its sharp onset divides clearly a MR peak into regions with strong (i.e., with the strength to cause the domain distributions of the FM layers in a FM/I/FM structure different from those of the individual FM layers) and weak interaction. The weak interaction regions (H beyond the coercivities) should give more stable MR responses for field sensing but the sensitivity was lower (our earlier analysis showed that the steep edge was due to the presence of AF interaction). In the other region, the AF effect can be so strong that the magnetizations arrange themselves antiferromagnetically even without change in applied field. We have observed such a phenomenon in our Fe/Al₂O₃/CoFe junctions with 3 extra Al₂O₃ layers. In the experiment, we took the junction out of the applied field to a zero-field environment in less than a second during a magnetic cycling. The subsequent response of the junction resistance (or MR) was observed. Figure 8 showed a comparison between the MR peak obtained in a magnetic cycling and the MR values attained in about 20 s after the junction was withdrawn to a zero-field environment. Starting from the left of the peak, in Region 1 ($H < -140$ Oe, note that H_c of CoFe is 156 Oe), the MR values rose to about 1.6%, slightly higher than the zero-field value (1.37%). This can be explained as follows: For $H > H_c$ of CoFe, AF interaction was weak. So when the junction was withdrawn from the field, the MR values tended to the zero-field value of 1.37%. However, since the field decreased from $H > 140$ Oe to zero, it passed the AF region (regions 2 and 3, between the coercivities) and allowed a chance for AF interaction to take place. The result was that the small AF interaction raised the MR slightly from 1.37% to 1.6%. In region 2 ($H_{\text{peak}} = H = -140$ Oe), the MR values rose far beyond the zero-field value and if H was near H_{peak} , the MR values were even

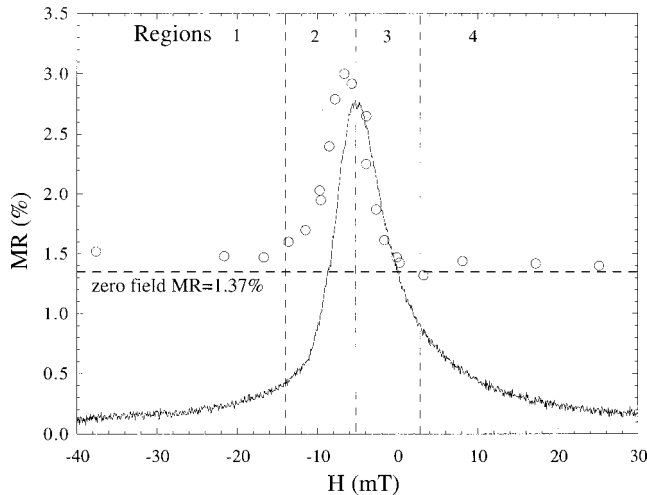


FIG. 8. Comparison of the MR curve obtained in a continuous magnetic cycling to the MR values attained in about 20 s after the Fe/Al₂O₃/CoFe junction was abruptly withdrawn to a zero-field environment.

higher than MR_{peak} . This was obviously due to the strong AF interaction occurring when H went between the coercivities. The interaction tended to align the FM electrode antiferromagnetically and caused instability to the magnetic alignment. Therefore the MR response to external field was unstable in region 2. In region 3 ($H_{\text{peak}} = H = 30$ Oe, note that H_c of Fe is 40 Oe) on the right-hand side of the peak, MR did not respond to the sudden field reduction. Again it was the AF effect that held the magnetic alignment (thus the MR) when H vanished. In region 3, the MR values stayed (or slightly reduced) without going up as in region 2 because H was leaving the strong AF region instead of entering. For region 4 ($H = 30$ Oe), H vanished without passing into the AF region, and therefore MR rested near the zero-field value of 1.37%. The above discussion shows the importance of magnetic interaction between the FM layers in the dynamic response of the junction MR.

V. DISCUSSION AND SUMMARY

The analysis in this paper challenges some common beliefs in the behavior of FM-I-FM junctions: (i) We have shown that the peak MR may not be the highest possible value because the magnetizations are not necessarily completely antiparallel to each other. As mentioned in Sec. II, the model suggested that the domain alignment is sensitive to temperature, and therefore the incomplete AF configuration at the peak can be one of the causes of the temperature dependence of MR. (ii) The shape of the MR curves, especially

near the peak, is mainly governed by the AF interaction of the FM layers, rather than the magnetization behavior of individual FM layers. Also single domain structure is not essential for a MR peak to have flat top and steep edges. Furthermore, a wider separation of the coercivities does not necessarily give a higher peak MR, because a strong AF interaction alone is adequate for antiparallel alignment of the magnetizations. Low MR values in some junctions (e.g., the Ni/Al₂O₃/Co junctions in Ref. 21) may be a consequence of lack of AF interaction, in addition to other factors. In such cases, an insulator with high magnetic permeability around the junction areas will help in getting higher MR values by promoting AF interaction. (iii) The MR value may not be temporally stable for magnetic-field measurement due to the presence of AF interaction.

In the derivation of the model, we have not taken into account the tunneling involving domain-wall regions. Within the width of the walls, the magnetizations may have components normal to the plane of the FM layers, in contrast to our assumption that magnetizations are in-plane. We deal with this problem by comparing the simulation of MR- H curves at high field and at low field before the AF interaction became significant. We have shown in Sec. III that the measured and the simulated MR were well in a direct proportionality at both high and low fields, with same proportional constants. At high field (beyond the saturation field), the total area of domain-wall regions should be small compared to low field cases (especially near the coercivities). The conclusion is that domain-wall regions do not have much effect on the simulation. The reason is that the proportion of spin conserved tunneling involving domain walls is small since the probability for an electron in the wall to see a state with same spin direction on the other side of the barrier is relatively small.

In summary, we have derived the multidomain model for the MR behavior of FM-I-FM tunnel junctions. The validity of the model was proved by the satisfactory explanations of the features of MR- H curves. On the application side, it provides a more quantitative way to study the AF interaction in FM-I-FM structures. The analysis in Sec. IV showed the significance of AF interaction on the field sensing ability of ferromagnetic junctions. Moreover Eqs. (6) and (7) provide the tools for quantitative analysis of the dependence of MR on temperature which is a parameter of the magnetization of individual FM layers.

ACKNOWLEDGMENT

P. K. Wong would like to thank the Croucher Foundation of Hong Kong for supporting his research in Cambridge University.

¹M. Julliere, Phys. Lett. **54A**, 225 (1975).

²J. C. Slonczewski, Phys. Rev. B **39**, 6995 (1989).

³T. Yaoi, S. Ishio, and T. Miyazaki, J. Magn. Magn. Mater. **126**, 430 (1993).

⁴T. Miyazaki and N. Tezuka, J. Magn. Magn. Mater. **151**, 403 (1995).

⁵J. S. Moodera, L. R. Kinder, T. M. Wong, and R. Meservey, Phys. Rev. Lett. **74**, 3273 (1995).

⁶J. S. Moodera, J. Nowak, and R. J. M. Veerdonk, Phys. Rev. Lett. **80**, 2941 (1998).

⁷S. S. P. Parkin, R. E. Fontana, and A. C. Marley, J. Appl. Phys. **81**, 5521 (1997).

- ⁸S. T. Chui, Phys. Rev. B **55**, 5600 (1997).
- ⁹S. Zhang, P. M. Levy, A. C. Marley, and S. S. P. Parkin, Phys. Rev. Lett. **79**, 3744 (1997).
- ¹⁰X. Zhang, B. Z. Li, and F. C. Pu, Phys. Lett. A **236**, 356 (1997).
- ¹¹J. Inoue and S. Maekawa, Phys. Rev. B **53**, R11 927 (1996).
- ¹²A. M. Bratkovsky, Phys. Rev. B **56**, 2344 (1997).
- ¹³J. Mathon, Phys. Rev. B **56**, 11 810 (1997)
- ¹⁴J. M. MacLaren, X. G. Zhang, and W. H. Butler, Phys. Rev. B **56**, 11 827 (1997).
- ¹⁵J. Nowak and J. Rauluszkiewicz, J. Magn. Magn. Mater. **109**, 79 (1992).
- ¹⁶S. A. Rishton, Y. Lu, R. A. Altman, A. C. Marley, X. P. Bian, C. Jahnes, R. Viswanathan, G. Xiao, W. J. Gallagher, and S. S. P. Parkin, Microelectron. Eng. **35**, 249 (1997).
- ¹⁷P. K. Wong, J. E. Evetts, and M. G. Blamire, Appl. Phys. Lett. **73**, 384 (1998); P. K. Wong, J. E. Evetts, and M. G. Blamire, J. Appl. Phys. **83**, 6697 (1998).
- ¹⁸S. Chikazumi, *Physics of Ferromagnetism*, 2nd ed. (Oxford University, New York, 1997).
- ¹⁹D. J. Craik, *Structure and Properties of Magnetic Materials* (Pion Limited, London, 1971).
- ²⁰D. Jiles, *Introduction to Magnetism and Magnetic Materials*, 1st ed. (Chapman & Hall, London, 1991).
- ²¹Y. Suezawa, F. Takahashi, and Y. Gondo, Jpn. J. Appl. Phys., Part 2 **31**, L1415 (1992).
- ²²D. Paraskevopoulos, R. Meservey, and P. M. Tedrow, Phys. Rev. B **16**, 4907 (1977).
- ²³H. Tsuge and T. Mitsuzuka, Appl. Phys. Lett. **71**, 3296 (1997).